ASTRONOMY & ASTROPHYSICS
SUPPLEMENT SERIES

Astron. Astrophys. Suppl. Ser. **120,** 275-282 (1996)

Light curves and periods of Mira variables*,**,***,†

C. Alard[1,2], A. Terzan[3] and J. Guibert[1,2]

[1] Centre d'Analyse des Images CNRS/INSU/MAMA, Observatoire de Paris, France
[2] Observatoire de Paris (DEMIRM)/URA 336 du CNRS, 77, Avenue Denfert-Rochereau F-75014 Paris, France
[3] Observatoire de Lyon (CRAL), F-69561 Saint Genis Laval Cedex, France

Received April 7, 1995; accepted April 9, 1996

Abstract. — Good distance indicators are needed in studies of the galactic structure. Pulsating variables can be used, but the problem is to find a homogenous sample obeying a period-luminosity relation with low scatter. In this paper, we show how such a sample can be produced using the Terzan catalogue of Variables and available Schmidt plates. We have selected 150 large amplitude variables discovered by Terzan in a field of 25 sq degrees near the Galactic Centre. A set of 22 red plates was scanned with the MAMA machine, providing time series for all the variables. The times series were analysed using both the periodogram and Renson's method. Periods could be derived for 122 stars of the sample showing clearly that most of these objects are Miras. As a conclusion we show that with some infrared photometry, these Miras could be used as good distance indicators in this region.

Key words: stars: AGB — infrared: stars — Galaxy: centre

1. Introduction

1.1. *AGB stars as probes of the galactic structure*

As demonstrated by Weinberg (1992), AGB stars can be very useful for the study of galactic structure. Weinberg used the variable stars of the IRAS survey (1988), and making the assumption that most of these objects are AGB stars having the same absolute magnitude, he could derive their spatial distribution. After correction for distance incompleteness, the IRAS variables traced a structure where the bulge was found as being elongated, and the beginning of two spiral arms was visible. This demonstrates the power of the method. However, the absolute K or bolometric magnitude of galactic AGB stars depends on the period (see, e.g., Whitelock et al. 1991; Glass et al. 1995, and references therein). For Miras, with such a P-L relation, Weinberg's hypothesis according to which all Miras have the same absolute magnitude may produce a scatter of about 0.5 mag.

Taking into account the aforementioned period-luminosity relations, it might be possible to reduce this scatter, which will allow a better analysis of the galactic structure. goal of this study is to produce, from a set of available Schmidt plates, a sample of periodic AGB variables (Miras), with periods suitable to the derivation of the absolute luminosity and hence the distance of each object. However, both K and bolometric magnitudes involve infrared photometry, so our work should be further completed with observations in this spectral region.

1.2. *Miras*

Mira stars are large amplitude variables (more than 2 mag in the visible for most of them) with long periods (from 150 to 500 days). In the HR diagram they are located on the AGB branch, a region occupied by old giant stars. These represent a late stage in the evolution of intermediate mass objects, connected with high mass loss rate leading to PN formation. Due to the intrinsic colours of these objects, red plates are very well suited for these variables. A long time basis covering a sufficient number of periods is also needed for period finding.

Our collection includes a set of 22 ESO red plates taken between 1980 and 1992. They cover the central part of the 10 × 10 degrees field in which one of us (A. T.), using the blink microscope technique, had discovered several thousands of variables (Terzan & Gosset 1991 and references therein). Unfortunately, the time sampling is quite

Send offprint requests to: C. Alard
*Plate scanning done with MAMA. MAMA is developed and operated by INSU (Institut National des Sciences de l'Univers)
**Based on observations made at the European Southern Observatory, La Silla, Chile
***Table 3 only available in electronic form at CDS via anonymous ftp cdsarc.u-strasbg.fr or 130.79.128.5
†Figure 5 only available in electronic form at http://ww.edphys.fr

uneven. Consequently, irregular or semi-regular variables, for which it is impossible to fold all the measurements on a single cycle, are excluded from the present study.

2. Data reduction

2.1. *Scanning of the plates, and photometric calibration*

The MAMA machine was used in the mode in which it produces a digitised image of a small field centered on each of Terzan's stars. The magnitude determination was performed for the 22 red plates using a multi-threshold technique. Each plate was first calibrated by means of 55 standards (Terzan et al. 1982). For this purpose, a polynomial fit between photoelectric magnitudes and integrated photographic densities was made, for each threshold, with a least squares technique. Then, at each threshold where a given variable was detected and found as separated from possible neighbours, a magnitude was derived from the polynomial calibration. Finally, for each object and for each plate, the magnitudes obtained at the different thresholds were subsequently averaged.

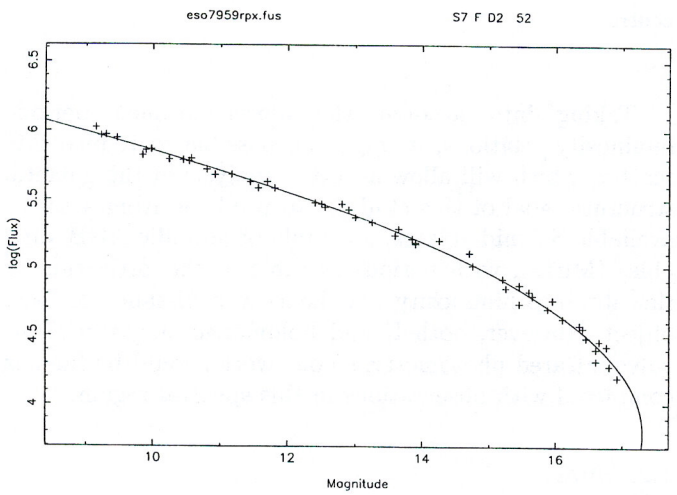

Fig. 1. Example of photometric calibration. "Flux" stands for the integrated photographic density

Table 1. Estimation of photometric errors

R magnitude	magnitude error
10 – 12	0.15
12 – 14	0.10
14 – 16	0.15
16 – 18	0.20

An estimate of the photometric accuracy can be derived from the residuals of the sequence fitting (Fig. 1) and the differences between the magnitudes obtained at the various thresholds. This estimate is given in Table 1 as a function of the R magnitude.

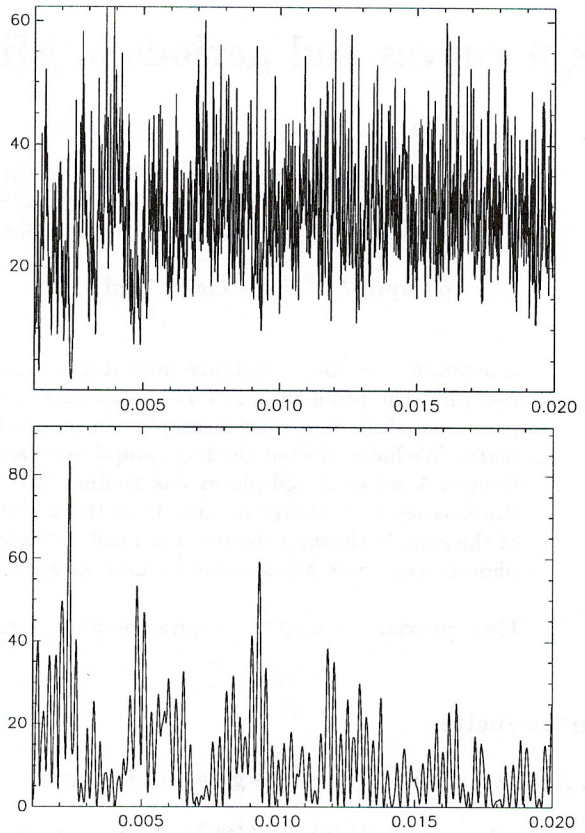

Fig. 2. Example of period determination. Top: Renson's method (θ_1); bottom: periodogram ($P_X(\omega)$)

2.2. *Period determination*

The limited number of points as well as their very uneven time spacing, sometimes results in poor sampling of the light curve. In such a case, comparative studies demonstrate that Renson's (1978) method generally works better, but gives no estimate of the probability that the tested signal is really periodic. To estimate this probability it is well known that a Fourier method, like the periodogram (Deeming 1975; Scargle 1982) is optimal (Swingler 1989). So we preferred to use both Renson's and the periodogram methods to analyse the data.

In Figs. 2 and 3, we give an example of a time series analysis. The frequency spectra estimated with Renson's and the Periodogram methods are plotted in Fig. 2. The minimum of θ_1 (Renson 1978), and the maximum of $P_X(\omega)$ (Scargle 1982), are obtained at values of the frequency very close to 0.002366 day^{-1}, leading to a period of 422.6 ±2 days. The derived phase diagram can be seen in Fig. 3.

Table 2. Miras found in the IRAS Point Source Catalog (PSC)

Terzan	PSC	period(d)	$\Delta\alpha''$	$\epsilon\alpha''$	$\Delta\delta''$	$\epsilon\delta''$	12μ	25μ	$\log(S_{12}/S_{25})$	I_V
Ter0051	17159-2954	298.7	-10.4	44	-0.5	6	1.020	0.717	0.153	0
Ter0060	17163-2917	307.3	-10.4	38	-1.9	6	2.992	1.531	0.291	9
Ter0070	17168-2856	523.6	-03.9	28	-0.3	6	15.27	6.673	0.360	9
Ter0098	17183-2838	286.4	-03.9	30	0.2	5	2.480	1.303	0.280	8
Ter0105	17186-2914	422.7	03.9	25	-1.6	5	14.07	5.470	0.423	9
Ter0146	17201-2859	387.9	-05.2	28	0.2	5	3.739	1.857	0.304	9
Ter0244	17241-2921	435.9	05.2	41	-1.1	7	2.529	1.467	0.237	9
Ter0249	17242-3045	404.5	-03.9	31	4.4	5	6.929	5.037	0.138	1
Ter0411	17268-3141	517.6	10.4	41	6.6	8	8.789	4.836	0.259	9
Ter0574	17303-2955	305.1	09.1	39	1.4	6	4.130	2.709	0.183	9
Ter0603	17321-3053	438.6	03.9	48	1.8	9	10.69	5.725	0.271	8
Ter0605	17322-3111	222.5	19.5	35	0.9	8	2.586	1.878	0.139	

Ter = Terzan Number (Terzan et al. 1982); $\Delta\alpha = \alpha$(IRAS)-α(Terzan); $\Delta\delta = \delta$ (IRAS)-δ(Terzan)
$\epsilon\alpha$ and $\epsilon\delta$ are the dimensions of the IRAS error box (95 % confidence)
I_V (Variability Index) is the probability that 12μ and 25μ fluxes showed correlated variations
($\epsilon\alpha$, $\epsilon\delta$, 12μ, 25μ and I_V are taken from the IRAS PSC)

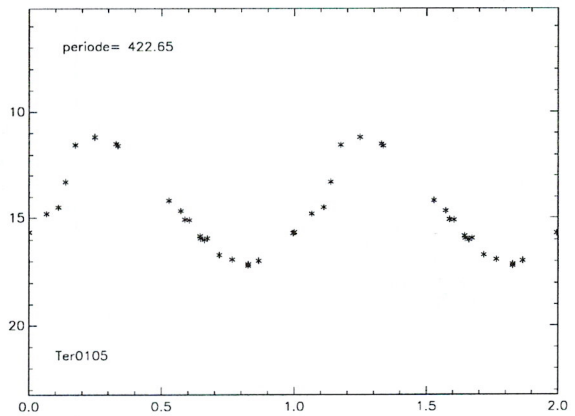

Fig. 3. Phase diagram using the period determinations shown in Fig. 2

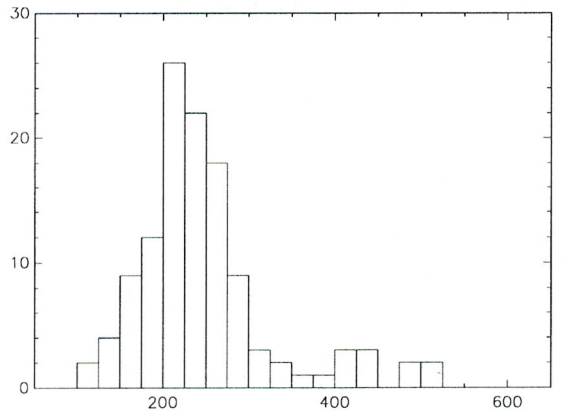

Fig. 4. Period Distribution of the Miras of our sample (periods are expressed in days)

The 150 times series were processed (Alard et al. 1993; Alard 1994), providing estimates of the period for each object, and the false alarm probability (Scargle 1982). Only the stars having a false alarm probability less than 5 percent, and a good agreement between the period estimates by Renson's and the Periodogram methods, were selected. A total of 122 objects satisfied these two conditions. The data are presented in Table 3. The phase diagrams are reproduced in Fig. 5. The common origin of the abscissae corresponds to the Julian date J.D. 2 443 966.58 (Astronomical Almanach, M6)

3. Comparison with the IRAS point source catalog

We have found 122 stars with quite regular and repetitive variations, which are therefore considered as being Miras. Usually these objects have circumstellar shells emitting in the far infrared. A total of 12 stars were found to lie in the error box of an IRAS source. In Table 2, the ratio $\log(S_{12}/S_{25})$, comprised between 0.1 and 0.5, agrees well with the expected values for Miras (see, e.g., Vardya et al. 1986). Moreover, 10 objects, over a total number of 12, have a variability probability exceeding 0.8 in the PSC. The number of IRAS observations for the two remaining LPVs (Ter0051 and Ter0605) was probably insufficient to suggest infrared variability. It could be rather surprising to find less than 10% of our (122) Miras in the IRAS PSC. However, there are two major reasons for the incompletness of the IRAS catalog in this region: the crowding on the one part, and the limited sensitivity of the survey on the other part.

4. Conclusions

Figure 4 shows that most of our stars are in the period range 150 to 300 days. The period-luminosity relations

derived from infrared photometry (Whitelock et al. 1991; Glass et al. 1995), are quite accurate for this range of periods (sigma ≈ 0.2 mag). Using the period as derived above from the optical measurements, the absolute magnitude K_0 can be obtained. On the other hand, the mean apparent J and K magnitudes can be derived from infrared measurements . The extinction in this field is high in the visible, and probably also in the infrared. But the relation between the period and the color index $(J-K)_0$ (Glass et al. 1995), will give us the dereddened color, allowing us to derive both the extinction and distance modulus.

With this sample of stars, we demonstrate the interest of studying LPVs. This work will be continued for the other Terzan fields and, with the addition of some new plates, could be extended to variables of all types.

Acknowledgements. We are grateful to the MAMA team for assistance during the scans, to L. Pagani for providing the multithreshold algorithm, and to M. Feast for fruitful discussions. We also thank the referee (Dr. C. Sterken) for valuable comments and suggestions.

References

Alard C., 1994, Ap&SS 217, 155
Alard C., Terzan A., Guibert J., 1993, The Messenger 73, 31
Deeming T.J., 1975, Ap&SS 36, 137
Glass I.S., Whitelock P.A., Catchpole R.M., Feast M.W., 1995, MNRAS 273, 383
Infrared Astronomical Satellite, NASA, Washington, DC
Renson P., 1978, A&A 63, 125
Scargle D.J., 1982, ApJ 263, 835
Swingler D.N., 1989, AJ 97, 280
Terzan A., Bijaoui A., Ju K.H., Ounnas C. 1982, A&AS 49, 715
Terzan A., Gosset E., 1991, A&AS 90, 451
Vardya M.S., De Jong T., Willems F.J., 1986, ApJ 304, L32
Weinberg D.J., 1992, ApJ 384, 81
Whitelock P.A., Feast M.W., Catchpole R., 1991, MNRAS 248, 276

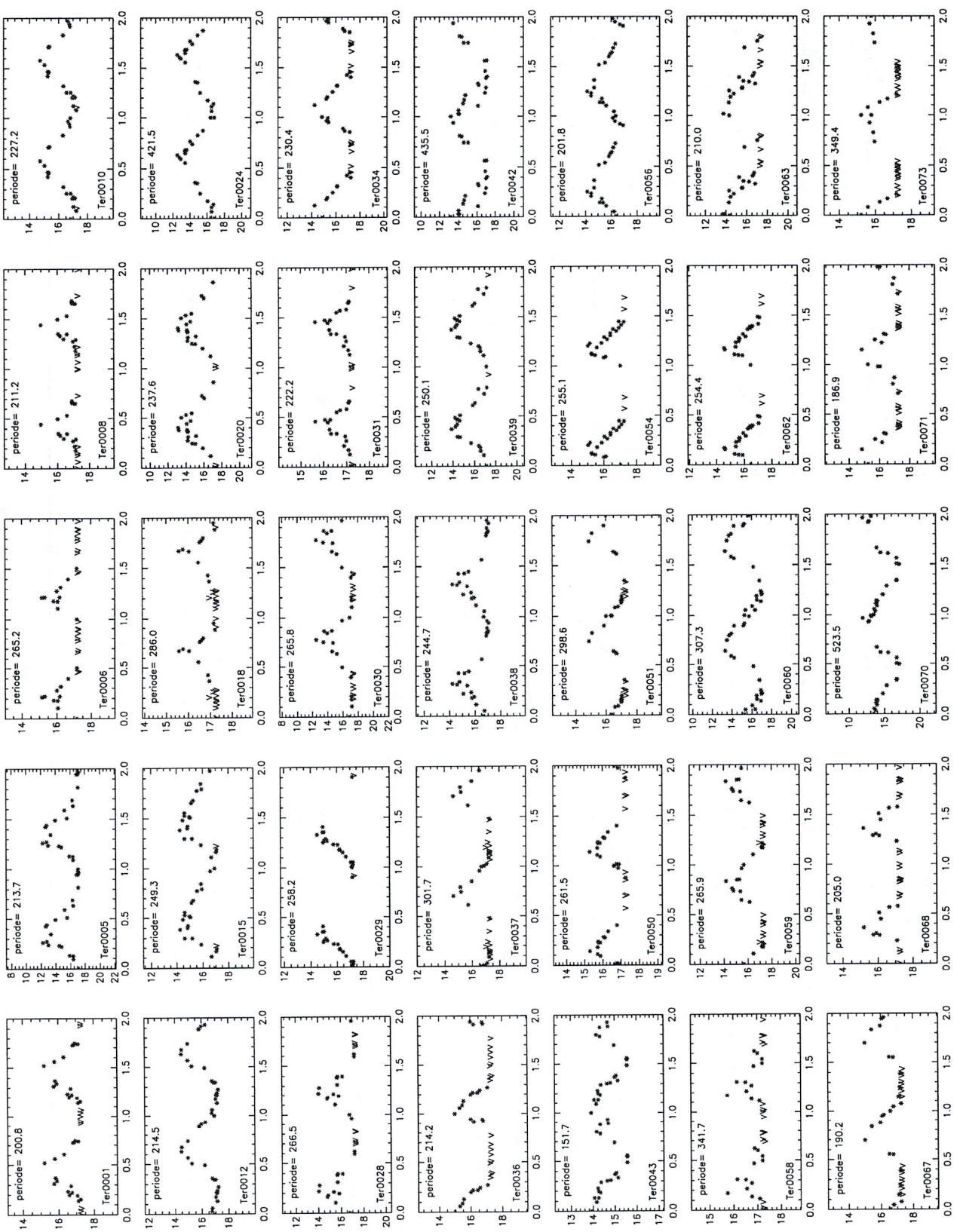

Fig. 5. Light curves of the Miras (only in electronic form)

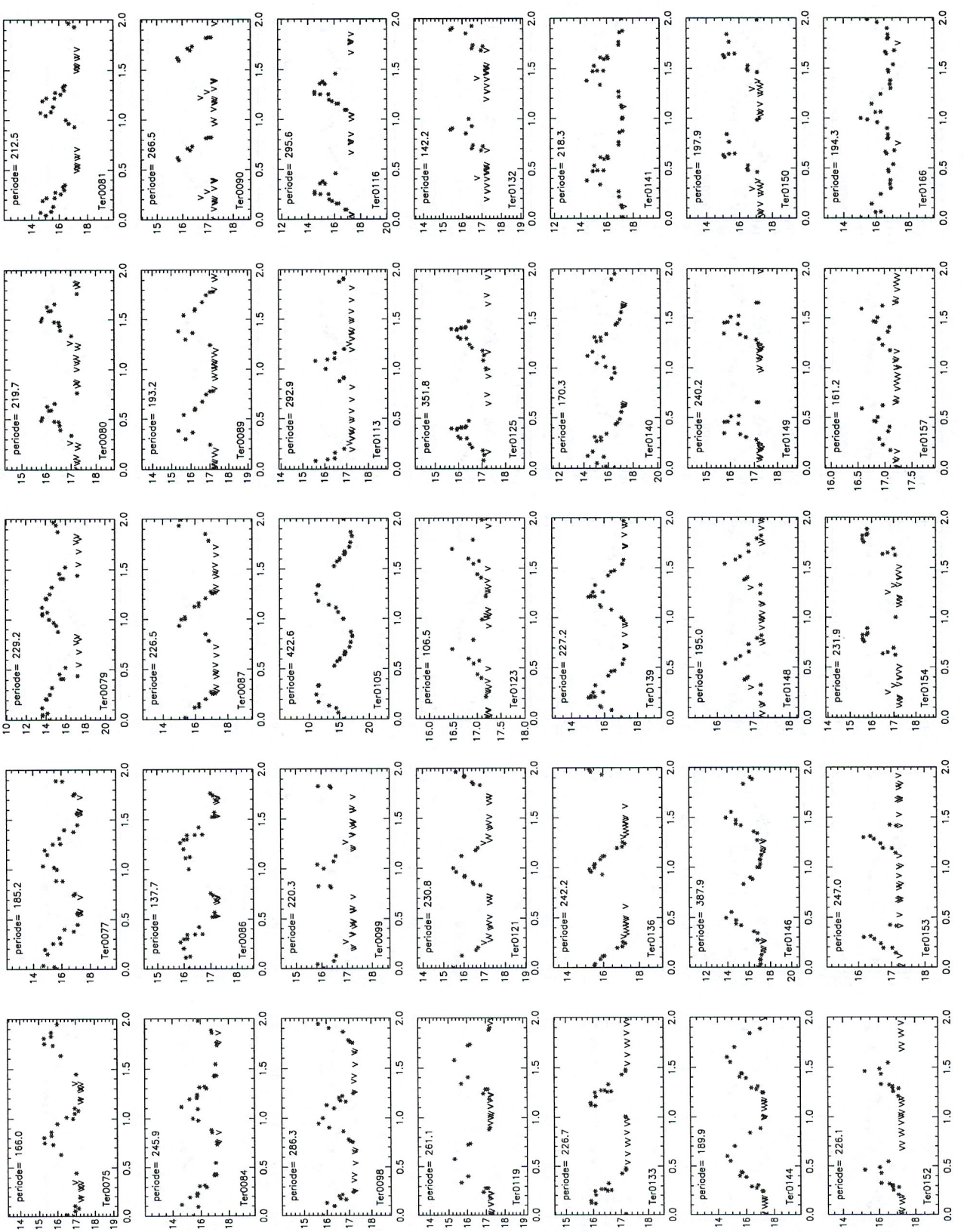

Fig. 6. continued (only in electronic form)

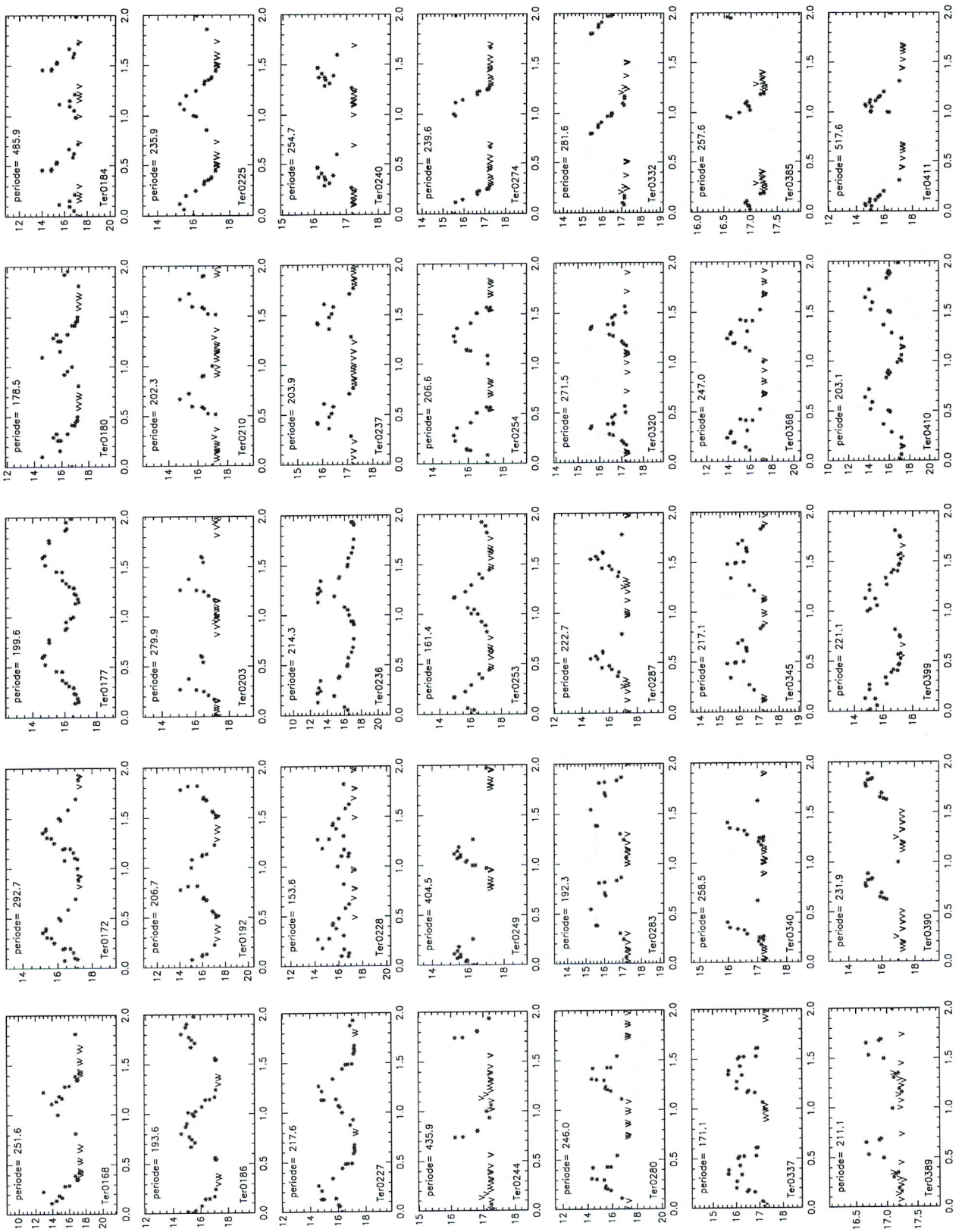

Fig. 7. continued (only in electronic form)

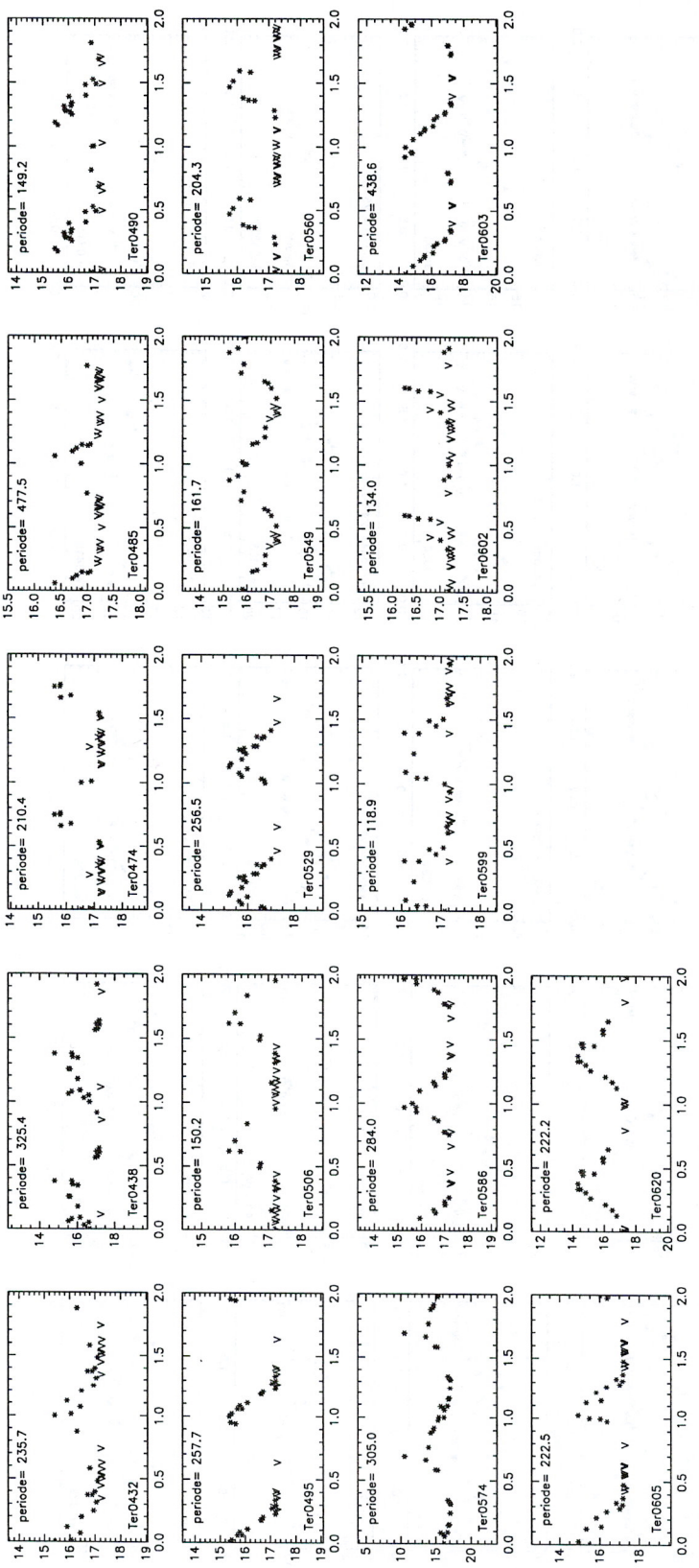

Fig. 8. continued (only in electronic form)